# Efficient and Accurate Sampling of the Thermal Neutron Scattering Law in OpenMC

by

Amelia J. Trainer

SUBMITTED TO THE DEPARTMENT OF NUCLEAR SCIENCE AND ENGINEERING IN PARTIAL FULFILLMENT OF THE REQUIREMENTS FOR THE DEGREE OF

BACHELOR OF SCIENCE IN NUCLEAR SCIENCE AND ENGINEERING

AT THE

MASSACHUSETTS INSTITUTE OF TECHNOLOGY

JUNE 2019



Signature of Author:_____

Amelia J. Trainer
Department of Nuclear Science and Engineering
May 18, 2019

Certified by:_____

Benoit Forget
Associate Professor of Nuclear Science and Engineering
Thesis Supervisor

Accepted by:_____

Michael Short
Assistant Professor of Nuclear Science and Engineering
Chairman, NSE Committee for Undergraduate Students

# Efficient and Accurate Sampling of the Thermal Neutron Scattering Law in OpenMC

by

Amelia J. Trainer

Submitted to the Department of Nuclear Science and Engineering on May 18, 2019 in Partial Fulfillment of the Requirements for the Degree of Master of Science in Nuclear Science and Engineering

ABSTRACT

THIS IS MY ABSTRACT LOCATED IN TITLEPAGE.TEX

Thesis Supervisor: Benoit Forget
Title: Associate Professor of Nuclear Science and Engineering

Thesis Reader: Kord Smith
Title: Korea Electric Power Company (KEPCO) Professor of the Practice of Nuclear Science and Engineering

# Acknowledgements

Thanks

# Contents

# List of Figures

# List of Tables

# Chapter 1

# Introduction

## 1.1 Motivation

The merit of a nuclear system simulation is heavily dependent on the accuracy of the input nuclear data. Nuclear data (such as cross sections, particle emissions, etc.) is often complicated and highly energy dependent, which poses a challenge for those interested in effcieiently simulating the behavior of a nuclear system. Nuclear data is released in "evaluations", which are prepared by statistically combining experimentally measured data with theoretical predictions. The most widely used format for these evaluations is called the Evaluated Nuclear Data File (ENDF) [1]. ENDF files are generally not directly used by nuclear simulations, but are rather preprocessed to account for simulation-specific conditions. In doing so, the ENDF is converted into a more usable form, called "a compact ENDF" (ACE) [2].

Currently, the most widely trusted code used for nuclear data preprocessing is NJOY, which has been developed and maintained at Los Alamos National Lab (LANL) since the early 1970's [3]. It has a large users base and is versatile for many nuclear data related tasks, including resonance reconstruction, Doppler-Broadening, multi-group cross section generation, and the preparation of thermal neutron scattering data. NJOY's capabilities are spread across 24 modules, each of which has a specified task. Two modules in particular, LEAPR and THERMR, handle the calculation and representation of thermal scattering from bound moderators. While the accuracy of thermal neutron scattering data can greatly dictate the quality of thermal reactor analysis and safety margin calculations, it remains a difficult problem, due to effects (molecular structure, neutron wavelength, described below) that are not apparent for higher neutron energies.

Both thermal neutron scattering and resonant neutron scattering are highly dependent on incoming neutron energy. However, thermal neutron scattering cross sections must also account for molecular structure, since the energy of the incoming neutron is generally on the order of the molecules' excitation modes (i.e. below 1-10 eV). Excitation of these excitation modes can result in vibration, translation, or rotation of the target. Vibrational modes, also called phonons, are a primary concern when describing neutron scattering in a solid. In addition to the molecular excitation, thermal neutrons data processing is further complicated by considering the long neutron de Broglie wavelength. When

a neutron has energy in the thermal region, its wavelength can be on the order of the interatomic spacing, which allows it to interact with multiple nuclei, as opposed to a single atom [4].

Despite the above complications, a thermal scattering relationship $S(\alpha, \beta, T)$ is constructed to relate unitless neutron momentum and energy exchange ($\alpha$ and $\beta$, respectively) with the double differential inelastic incoherent scattering cross section $\sigma\left(E \rightarrow E', \mu\right)$. Once $S(\alpha, \beta, T)$, also called the "scattering law", is obtained, the cross section can be obtained using

$$\sigma\left(E \rightarrow E', \mu\right) = \frac{\sigma_b}{2k_bT}\sqrt{\frac{E'}{E}}S(\alpha, \beta, T), \tag{1.1}$$

where $\sigma_b$ is the characteristic bound scattering cross section of the target isotope, and $k_b$ is Boltzmann's constant and $T$ is the temperature. As shown in Eq. 1.1, if $S(\alpha, \beta, T)$ can be accurately obtained, the differential inelastic incoherent scattering cross section $\sigma\left(E \rightarrow E', \mu\right)$ is simple to calculate. Thus, the quality of thermal nuclear system modeling is directly tied to the preparation of the scattering law.

## 1.2 Current Methods of Preparing $S(\alpha, \beta, T)$

### 1.2.1 Types of Thermal Neutron Scattering

As mentioned in Sec. 1.1, the most widely used code for nuclear data processing is NJOY, which through two of its modules (LEAPR and THERMR) has the ability to prepare thermal scattering data. In particular, LEAPR is used to create a $S(\alpha, \beta, T)$ table, while THERMR tabulates the scattering law into a convenient form for simulations to use. Since LEAPR primarily calculates $S(\alpha, \beta, T)$, it will be of primary focus for the rest of this section.

Thermal neutron scattering can be broken into elastic and inelastic parts, which can then be further separated into coherent and incoherent parts. Elastic thermal scattering implies no change in neutron energy. Note that this differs from elastic scattering off of a single particle, in that a thermal neutron will elastically scatter off of an entire lattice, which makes the effective mass of the target extremely large. Thermal inelastic scattering can result in neutron energy loss, which corresponds to target excitation. At these low energies, neutron up-scattering can also occur, which implies neutron energy gain, and corresponds to target de-excitation. Excitations can correspond to creation of vibrational modes (phonons), as well as the creation of translational or rotational modes. For a system of particles with randomly distributed spins, coherent scattering consists of interacting wave effects, whereas incoherent scattering consists solely of a sum of non-interacting waves[1].

For materials with randomly distributed crystallites, the form of coherent inelastic scattering nearly equals that of incoherent inelastic scattering. This allows the coherent and incoherent inelastic components to be combined into one inelastic contribution, an

[1]Materials such as cold hydrogen that do not have randomly distributed have additional effects, so they have be considered apart from this simple coherent/incoherent discussion.

approximation known as the "incoherent approximation" [3, 4]. Thus, LEAPR separates the scattering calculation into inelastic, coherent elastic, and incoherent inelastic. This project focuses on inelastic scattering, due to the predominant importance of neutron energy change.

### 1.2.2 Inelastic Thermal Neutron Scattering

Recall from Sec. 1.1 that the double differential inelastic cross section is defined as

$$\sigma\left(E \to E', \mu\right) = \frac{\sigma_b}{2kT}\sqrt{\frac{E'}{E}} S_{n.sym}(\alpha, \beta, T) \tag{1.1}$$

which describes a neutron with incoming energy $E$ scattering with cosine $\mu$ into energy $E'$. Recall again that $\sigma_b$ is the characteristic bound scattering cross section for the target, $k_b$ is Boltzmann's constant, and $T$ is the temperature. Note that $S_{n.sym}(\alpha, \beta, T)$ is the non-symmetric form of the scattering law, which will be further discussed in !!!!!!!!!!!!!!!!!!. Dimensionless momentum and energy transfer, $\alpha$ and $\beta$ respectively, are defined as

$$\alpha = \frac{E' + E - 2\mu\sqrt{E'E}}{AkT} \tag{1.2}$$

$$\beta = \frac{E' - E}{kT} \tag{1.3}$$

The symmetric scattering law $S_{n.sym}(\alpha, \beta)$ can be written as an integral across time in units of $\hbar/k_bT$ seconds, [THIS USES THE GAUSSIAN APPROXIMATION SO CHECK OUT Scattering of Slow Neutrons by a Liquid George H. Vineyard]

$$S_{n.sym}(\alpha, \beta, T) = \frac{1}{2\pi}\int_{-\infty}^{\infty} \mathrm{e}^{i\beta\hat{t}}\mathrm{e}^{-\gamma(\hat{t})}\, d\hat{t} \tag{1.4}$$

where

$$\gamma(\hat{t}) = \alpha\int_{-\infty}^{\infty} P(\beta)\left[1 - \mathrm{e}^{-i\beta\hat{t}}\right]\mathrm{e}^{-\beta/2}\, d\beta \tag{1.5}$$

and

$$P(\beta) = \frac{\rho(\beta)}{2\beta\sinh(\beta/2)}. \tag{1.6}$$

Note that $\rho(\beta)$ is the phonon distribution or excitation frequency spectrum characteristic to the material, and that it normalizes to unity,

$$\int_0^{\infty} \rho(\beta)d\beta = 1. \tag{1.7}$$

Note that to get to this point, the only assumption made is that equating the form of incoherent inelastic scattering with that of coherent elastic scattering (incoheren approximation). At this point, LEAPR decomposes the frequency spectrum $\rho(\beta)$,

$$\rho(\beta) = \sum_{j=1}^{\#\ \text{osc.}} \omega_j\delta(\beta_j) + \rho_s(\beta) + \rho_t(\beta)) \tag{1.8}$$

into a sum of discrete oscillators (represented by weighted delta-functions $\omega_j\delta(\beta_j)$), a solid-type spectrum $\rho_s(\beta)$, and a translational spectrum $\rho_t(\beta)$. The solid-type spectrum and translational spectrum integrate to $\omega_s$ and $\omega_t$, respectively, such that

$$\sum_{j=1}^{\#\text{ osc.}} \omega_j + \omega_s + \omega_t = 1. \tag{1.9}$$

LEAPR uses each component of this decomposed frequency distribution to create a corresponding scattering law $S_{sym,i}(\alpha,\beta,T)$, then convolves these individual scattering laws to retreive the true scattering relation $S_{n.sym}(\alpha,\beta,T)$.

### Solid-Type Continuous Spectra

The solid-type continuous conribution to $S_{n.sym}(\alpha,\beta,T)$ can be calculated by representing Eq. 1.4 as a sum, and using a finite number of terms of that sum to approximate a contribution value. The solid-type continuous spectra depends on the frequency distributino $\rho(\beta)$. Eq. 1.5 can be rewritten as

$$\gamma(\hat{t}) = \alpha\lambda_s - \alpha\int_{-\infty}^{\infty} P(\beta)\mathrm{e}^{-\beta/2}\mathrm{e}^{-i\beta\hat{t}}\,d\beta. \tag{1.10}$$

where $\lambda_s$, known as the Debye-Waller coefficient for the solid-type spectra, is defined as

$$\lambda_s = \int_{-\infty}^{\infty} P(\beta')e^{-\beta'/2}\,d\beta'. \tag{1.11}$$

Thus, the exponential of Eq. 1.10 is

$$\mathrm{e}^{-\gamma(\hat{t})} = \sum_{n=0}^{\infty}\left(\mathrm{e}^{-\alpha\lambda_s}\frac{1}{n!}\left[\alpha\int_{-\infty}^{\infty} P(\beta')\mathrm{e}^{-\beta'/2}\mathrm{e}^{-i\beta'\hat{t}}\,d\beta'\right]^n\right) \tag{1.12}$$

where the exponential of the latter term has been represented as a Taylor series. The above can be used in Eq. 1.4, yielding

$$S_{n.sym}(\alpha,\beta,T) = \frac{1}{2\pi}\int_{-\infty}^{\infty}\mathrm{e}^{i\beta\hat{t}}\sum_{n=0}^{\infty}\left(\mathrm{e}^{-\alpha\lambda_s}\frac{1}{n!}\left[\alpha\int_{-\infty}^{\infty} P(\beta')\mathrm{e}^{-\beta'/2}\mathrm{e}^{-i\beta'\hat{t}}\,d\beta'\right]^n\right)\,d\hat{t} \tag{1.13}$$

$$= \mathrm{e}^{-\alpha\lambda_s}\sum_{n=0}^{\infty}\frac{\alpha^n}{n!}\frac{1}{2\pi}\int_{-\infty}^{\infty}\mathrm{e}^{i\beta\hat{t}}\left[\int_{-\infty}^{\infty} P(\beta')\mathrm{e}^{-\beta'/2}\mathrm{e}^{-i\beta'\hat{t}}\,d\beta'\right]^n\,d\hat{t} \tag{1.14}$$

$$= \mathrm{e}^{-\alpha\lambda_s}\sum_{n=0}^{\infty}\frac{1}{n!}\left[\alpha\lambda_s\right]^n\mathcal{T}_n(\beta) \tag{1.15}$$

where

$$\lambda_s^n\mathcal{T}_n(\beta) = \frac{1}{2\pi}\int_{-\infty}^{\infty}\mathrm{e}^{i\beta\hat{t}}\left[\int_{-\infty}^{\infty} P(\beta')\mathrm{e}^{-\beta'/2}\mathrm{e}^{-i\beta'\hat{t}}\,d\beta'\right]^n\,d\hat{t}. \tag{1.16}$$

Note that

$$\mathcal{T}_0(\beta) = \delta(\beta) \tag{1.17}$$

and

$$\mathcal{T}_1(\beta) = \frac{1}{2\pi\lambda_s}\int_{-\infty}^{\infty} e^{i\beta\hat{t}}\int_{-\infty}^{\infty} P(\beta')e^{-\beta'/2}e^{-i\beta'\hat{t}}\,d\beta'\,d\hat{t} \tag{1.18}$$

$$= \frac{1}{2\pi\lambda_s}\int_{-\infty}^{\infty} P(\beta')e^{-\beta'/2}\int_{-\infty}^{\infty} e^{i(\beta-\beta')\hat{t}}\,d\hat{t}\,d\beta' \tag{1.19}$$

$$= \frac{1}{\lambda_s}\int_{-\infty}^{\infty} P(\beta')e^{-\beta'/2}\delta(\beta-\beta')\,d\beta' \tag{1.20}$$

$$= \frac{P(\beta)e^{-\beta/2}}{\lambda_s}. \tag{1.21}$$

As shown in Appendix A.1, $\mathcal{T}_n(\beta)$ can be attained using a convolution integral,

$$\mathcal{T}_n(\beta) = \int_{-\infty}^{\infty} \mathcal{T}_1(\beta')\,\mathcal{T}_{n-1}(\beta-\beta')\,d\beta'. \tag{A.8}$$

Solving the solid-type, continuous contribution to $S_{n.sym}(\alpha,\beta,T)$ can be done by computing $\mathcal{T}_i(\beta)$ for $i$ from 1 to a sufficiently large value of $n$. These $\mathcal{T}_i(\beta)$ values can be used in the Eq. 1.15, which directly contributes to $S_{n.sym}(\alpha,\beta,T)$.

### Discrete Oscillator

Shown in Fig. 1.1 is the phonon distribution for H in $H_2O$, as calculated by [5]. Often,

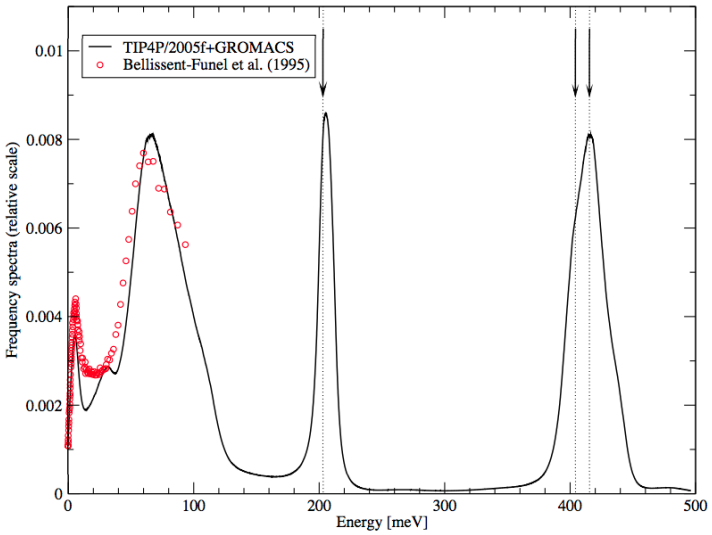


Figure 1.1: Phonon Distribution for H in $H_2O$ [5]. The red points and the arrows represent measured data against which to compare the calculated spectrum. Of particular interest are the two peaks near 200 and 400 meV, which are approximated in LEAPR as discrete oscillators.

vibrational modes appear as sharp peaks in the frequency distribution, and can be treated

as a weighted delta function at energy $E$, $\omega_i \delta_i(E)$. The corresponding

$$\mathcal{S}_i(\alpha,\beta) = \mathrm{e}^{-\alpha\lambda_i} \sum_{n=-\infty}^{\infty} \delta\left(\beta - n\beta_i\right) I_n\left[\frac{\alpha w_i}{\beta_i \sinh\left(\beta_i/2\right)}\right] \mathrm{e}^{-n\beta_i/2} \tag{1.22}$$

$$\mathcal{S}_i(\alpha,\beta) = \sum_{n=-\infty}^{\infty} A_{in}(\alpha)\delta\left(\beta - n\beta_i\right) \tag{1.23}$$

$$\lambda_i = w_i \frac{\coth\left(\beta_i/2\right)}{\beta_i} \tag{1.24}$$

where $\lambda_i$ is the Debye-Waller coefficient corresponding to the $i^{th}$ oscillator. When combining a continuous, solid-type spectrum with discrete oscillators, the total Debye-Waller coefficient is simply the sum,

$$\lambda = \lambda_s + \sum_{i=1}^{N} \lambda_i \tag{1.25}$$

where there are $N$ oscilllators considered.

**Translational Spectra**

## 1.3 Areas of Improvement

### 1.3.1 Input Phonon Distribution Approximations

### 1.3.2 Sampling from $S(\alpha, \beta, T)$

# Chapter 2

# Accurate Representation of Phonon Distributions

## 2.1 Discrete Oscillator Approximation for Phonon Spectra

Tell me why this is fundamentally different than the contin treatment. Actually go and walk through what NJOY manual is saying.

## 2.2 Representing Discrete Oscillators as Continuous Points in Freq. Dist.

### 2.2.1 Equivalence of Revised-LEAPR to Legacy-LEAPR

As part of this project, I rewrote LEAPR in C++. Look at these plots, I did a good job.

### 2.2.2 Representing Discrete Oscillator as a Thin Triangle in Freq. Dist.

This is where I want to put how $S(\alpha, \beta)$ looks for $\delta$ vs. triangle of width 2, for many alpha, beta pairs.

### 2.2.3 $S(\alpha, \beta)$ Response to Changes in Triangle Size

This is where I want to pick a few $\alpha$ values, and show how changing triangle size affects $S(\alpha, \beta)$

## 2.3 Nonuniform Phonon Distribution Energy Grid

# Chapter 3

# Improved Sampling of $S(\alpha, \beta)$

This is where I'm going to talk about Pavlou's paper

# Bibliography


[1] M Herman, Cross Sections Evaluation Working Group, et al. *ENDF-6 Formats Manual Data Formats and Procedures for the Evaluated Nuclear Data File ENDF/B-VI and ENDF/B-VII*. Tech. rep. Brookhaven National Laboratory (BNL) National Nuclear Data Center, 2009.

[2] *ADS Nuclear Data Library. ACE formatted Library for Accelerator Driven Systems*. https://www-nds.iaea.org/adsV1/adsace.html. [Online; accessed 7-December-2017]. 2005.

[3] Robert Macfarlane et al. *The NJOY Nuclear Data Processing System, Version 2016*. Tech. rep. Los Alamos National Laboratory (LANL), 2017.

[4] Jesse Curtis Holmes. "Monte Carlo Calculation of Thermal Neutron Inelastic Scattering Cross Section Uncertainties by Sampling Perturbed Phonon Spectra". PhD thesis. North Carolina State University, 2014.

[5] JI Marquez Damian, JR Granada, and DC Malaspina. *CAB models for water: a new evaluation of the thermal neutron scattering laws for light and heavy water in ENDF-6 format*. Tech. rep. 2014, pp. 280–289.

# Appendices

# Appendix A

# Background

## A.1 $T_n(\beta)$ Representation as a Convolution Integral

$$\mathcal{T}_n(\beta) = \frac{1}{2\pi}\frac{1}{\lambda_s^n}\int_{-\infty}^{\infty} \mathrm{e}^{i\beta\hat{t}} \left[\int_{-\infty}^{\infty} P(\beta')\mathrm{e}^{-\beta'/2}\mathrm{e}^{-i\beta'\hat{t}}\, d\beta'\right]^n \, d\hat{t}. \tag{A.1}$$

$$\mathcal{T}_n(\beta) = \frac{1}{2\pi}\frac{1}{\lambda_s^n}\int_{-\infty}^{\infty} \mathrm{e}^{-i\beta\hat{t}} \left[\int_{-\infty}^{\infty} P(\beta')\mathrm{e}^{\beta'/2}\mathrm{e}^{-i\beta'\hat{t}}\, d\beta'\right] \left[\int_{-\infty}^{\infty} P(\beta'')\mathrm{e}^{-\beta''/2}\mathrm{e}^{-i\beta''\hat{t}}\, d\beta''\right]^{n-1} \, d\hat{t} \tag{A.2}$$

$$\mathcal{T}_n(\beta) = \frac{1}{2\pi}\frac{1}{\lambda_s^n}\int_{-\infty}^{\infty}\int_{-\infty}^{\infty} \mathrm{e}^{-i\beta\hat{t}}P(\beta')\mathrm{e}^{\beta'/2}\mathrm{e}^{-i\beta'\hat{t}} \left[\int_{-\infty}^{\infty} P(\beta'')\mathrm{e}^{-\beta''/2}\mathrm{e}^{-i\beta''\hat{t}}\, d\beta''\right]^{n-1} \, d\beta'\, d\hat{t} \tag{A.3}$$

$$\mathcal{T}_n(\beta) = \frac{1}{2\pi}\frac{1}{\lambda_s^n}\int_{-\infty}^{\infty} \mathrm{e}^{-i\beta\hat{t}}P(\beta')\mathrm{e}^{\beta'/2}\int_{-\infty}^{\infty} \mathrm{e}^{-i\beta'\hat{t}} \left[\int_{-\infty}^{\infty} P(\beta'')\mathrm{e}^{-\beta''/2}\mathrm{e}^{-i\beta''\hat{t}}\, d\beta''\right]^{n-1} \, d\hat{t}\, d\beta' \tag{A.4}$$

$$\mathcal{T}_n(\beta) = \frac{1}{2\pi}\frac{1}{\lambda_s^n}\int_{-\infty}^{\infty} P(\beta')\mathrm{e}^{\beta'/2} \left[\int_{-\infty}^{\infty} \mathrm{e}^{i(\beta-\beta')\hat{t}} \left[\int_{-\infty}^{\infty} P(\beta'')\mathrm{e}^{-\beta''/2}\mathrm{e}^{-i\beta''\hat{t}}\, d\beta''\right]^{n-1} \, d\hat{t}\right] d\beta' \tag{A.5}$$

$$\mathcal{T}_n(\beta) = \int_{-\infty}^{\infty} \frac{P(\beta')\mathrm{e}^{\beta'/2}}{\lambda_s} \left[\frac{1}{2\pi\lambda_s^{n-1}}\int_{-\infty}^{\infty} \mathrm{e}^{i(\beta-\beta')\hat{t}} \left[\int_{-\infty}^{\infty} P(\beta'')\mathrm{e}^{-\beta''/2}\mathrm{e}^{-i\beta''\hat{t}}\, d\beta''\right]^{n-1} \, d\hat{t}\right] d\beta' \tag{A.6}$$

$$\mathcal{T}_n(\beta) = \int_{-\infty}^{\infty} \frac{P(\beta')\mathrm{e}^{\beta'/2}}{\lambda_s} \mathcal{T}_{n-1}\left(\beta-\beta'\right) d\beta' \tag{A.7}$$

$$\mathcal{T}_n(\beta) = \int_{-\infty}^{\infty} \mathcal{T}_1\left(\beta'\right) \mathcal{T}_{n-1}\left(\beta-\beta'\right) d\beta' \tag{A.8}$$